

TRIAXIAL ELASTO-PLASTIC AND FRACTURE MODEL FOR CONCRETE

Koichi MAEKAWA*, Jun-ichi TAKEMURA**,
Paulus IRAWAN*** and Masa-aki IRIE****

The complete constitutive equations in the form of tangential stiffness matrix are derived from incorporation of the constitutive law of the continuum fracture with the one of plasticity. The triaxial stress states are the main concern of authors since the accomplished model is wished to be a crucial and universal tool of analysis for laterally confined RC columns with wider variety of geometry and dimension. The constitutive equation derived under triaxial stresses was proved to cover the plastic and fracturing aspects of concrete as well as Von-Mises type of plasticity serving as the model of steel in reinforced concrete. The authors validated the fitness of the model for the triaxial behaviors of concrete reported. The failure envelope was not utilized in formulation unlike the theory of plasticity.

Keywords : constitutive law, plasticity, fracture, confinement

1. INTRODUCTION

The design oriented constitutive models for the fiber stress of flexural members confined by lateral reinforcement can be said as the spatially averaged model applicable to particular members. The local stress and strain induced by the three dimensional (3D) arrangement of the lateral steel has not been directly thought yet, but the mean stress versus mean strain relation has been main concern of practitioners¹³⁾. Accordingly, the spatially averaged stresses have included the spacing, shapes of lateral ties, the yield strength of steel and others¹⁴⁾. The averaged model can be estimated through laterally reinforced column tests subjected to uniform axial compression, but the mean fiber stress under the eccentric loads can not be found on this line. This spatially averaged constitutive model is convenient for member designs but simultaneously keeps the applicability narrow.

The other approach is to take into account the 3D local stress as it is, whatever the geometrical condition of lateral confinement would be specified. As long as the authors' knowledge, Inoue et al.¹⁾ firstly applied the finite element analysis to steel confined columns. This approach was very strategic whatever computational difficulty it has,

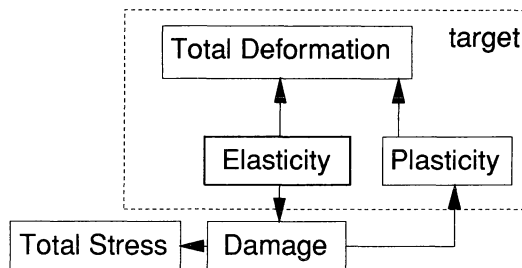


Fig.1 The entire scheme of formulation based on the elasto-plastic and fracture concept.

because its generality and versatility are fully attempted. The 3D computational evaluation of the strength and ductility of members definitely relies on the constitutive law of concrete under triaxial stresses. For realizing this generic method, the authors have proposed the continuum 3D fracture and plasticity constitutive laws^{2),3)} of the damaged continuum of concrete. This paper herein aims at the finalization of the general 3D constitutive equation by combining the elasticity, fracture and plasticity of concrete regarded as the damaged continuum in the frame of elasto-plastic and fracture concept as illustrated in Fig.1.

This paper will also serve to verify the complete constitutive equation based on the cyclic loading tests of concrete under triaxial stresses. Since the application of the model concerned is oriented to the laterally confined RC columns, the accuracy of the modeling will be checked mainly under comparatively small confinement condition.

2. FULL CONSTITUTIVE MATRIX

Concrete can be regarded as the damaged continuum with plasticity⁴⁾ as shown in Fig.2. The total

* Member of JSCE, Dr. Eng., Associate Professor, Dept. of Civil Engineering, The University of Tokyo (7-3-1, Hongo, Bunkyo-Ku, Tokyo 113).

** Member of JSCE, Ms. Eng., Ministry of Transport, Former Graduate Student of The University of Tokyo.

*** Graduate Student, Dept. of Civil Engineering, The University of Tokyo.

**** Member of JSCE, Ms. Eng., Civil Engineer, Nikken Sekkei, Former Graduate Student of The University of Tokyo.

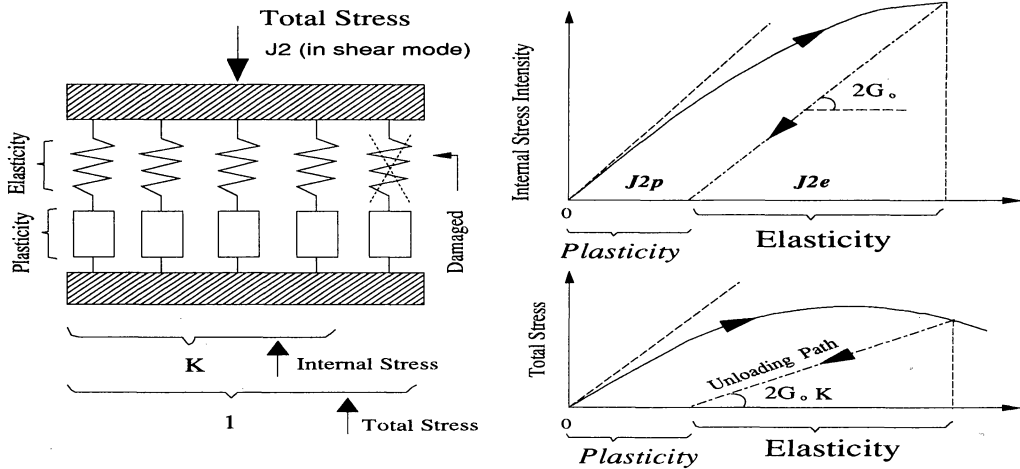


Fig.2 Schematic Elasto-plastic and Fracture System of Damaged Concrete

Table 1 Definition of Stress Intensity Indicators

Parameters	Total Stress Indicators	Internal Stress/Elasticity
Mean (1st Inv.)	$I_1 \equiv \frac{1}{3} \sigma_{kk}$	$I_{1e} \equiv \frac{1}{3} \epsilon_{ekk}$
Deviator (2nd Inv.)	$J_2 \equiv \sqrt{\frac{1}{2} s_{ij} s_{ij}}$	$J_{2e} \equiv \sqrt{\frac{1}{2} e_{eij} e_{eij}}$
Deviator (3rd Inv.)	$J_3 \equiv \sqrt{\frac{1}{3} s_{ij} s_{jk} s_{ki}}$	$J_{3e} \equiv \sqrt{\frac{1}{3} e_{eij} e_{ejk} e_{eki}}$
Deviator Tensor	$s_{ij} \equiv \sigma_{ij} - I_1 \delta_{ij}$	$e_{eij} \equiv \epsilon_{eij} - I_{1e} \delta_{ij}$

stress is idealized to be the sum of the internal stress developing in non-damaged constituent elements. It can be understood in Fig.2 that the elastic strain is directly proportional to the internal stress applied to active non-damaged elasto-plastic elements. Then, the elastic strain is assigned to represent the internal stress intensity which governs the plasticity and fracture of the continuum with defects²⁾⁻⁴⁾. The authors introduced the index to express the state and the intensity of the internal stress and the total stress as listed in Table 1.

The authors reported the effect of confinement on the fracture and plasticity of concrete under triaxial stress states. Brief summaries are coming as follows.

(1) *Fracture in hydrostatics* : The capacity of storing volumetric elastic strain energy is not damaged regardless of the magnitude of the defects induced in concrete and of the confinement denoted by I_{1e} ²⁾. With the volumetric elastic stiffness K_0 equal to $E_0/3(1-2\nu_0)$ where E_0 and ν_0 are elastic stiffness and Poisson's ratio, we have,

$$I_1 = 3K_0 I_{1e} \dots \dots \dots (1)$$

(2) *Fracture in shear* : The absorption of the shear elastic strain energy is degraded according to the state of load-induced fracture. The growth of the continuum damage denoted by the fracture parameter K is boosted by the internal shear stress intensity represented by J_{2e} and J_{3e} but suppressed by the confinement denoted by I_{1e} ²⁾. This correlation of I_{1e} , J_{2e} and J_{3e} concerning fracture is incorporated by the equivalent elasticity F as,

$$J_2 = 2G_0 K(F) J_{2e} \dots \dots \dots (2)$$

where, $F : F(I_{1e}, J_{2e}, J_{3e})$, G_0 : shear elastic stiffness equal to $E_0/2(1+\nu_0)$. Here, F in Eq.(2) is equal to F_{max} i.e., the maximum value of F in the past loading hysteresis. When the updated value of F is smaller than the past maximum value denoted by F_{max} the fracture does not proceed but remains stable. This is the fracture criterion.

(3) *Plasticity in shear* : The plastic deviator in shear is advanced by the internal shear stress intensity expressed by J_{2e} but not influenced by the magnitude of confinement³⁾. Therefore, this can be indicated by the plastic hardening function H as,

$$J_{2p} = H(J_{2e}) \dots\dots\dots (3)$$

where,

$$J_{2p} = \int \frac{\rho_{eij} d\varepsilon_{pji}}{2J_{2e}}$$

J_{2e} in Eq.(3) is equal to $J_{2e\max}$, i.e., the maximum value of J_2 in the past loading hysteresis. When J_{2e} is less than the maximum value regarded as the representative of the plastic history, no progress in plasticity is assumed. This is the plasticity criterion.

(4) *Plasticity in volume* : The volumetric plastic strain associated with the shear plasticity is significantly affected by the magnitude of the confinement indicated by I_{1e} . This nonlinearity is named the shear dilatancy³⁾ indicated by the dilatancy derivative D as,

$$dI_{1p} = D(I_{1e}, K) dJ_{2p} \dots\dots\dots (4)$$

where,

$$dI_{1p} = \frac{1}{3} d\varepsilon_{pkk}$$

The "effect of confinement", which has been of great interest, are classified into the continuum fracture and plasticity in terms of the volumetric and deviatoric aspects, respectively. The above four equations are cores of continuum fracture and plasticity constitutive laws. By solving Eq.(1) and Eq.(2) simultaneously, we have²⁾,

$$d\sigma_{ij} = M_{ijkl} d\varepsilon_{ekl} \dots\dots\dots (5a)$$

$$M_{ijkl} = 2G_0K\delta_{ik}\delta_{jl} + \frac{1}{3} \left[(3K_0 - 2G_0K)\delta_{ij} + 2G_0\rho_{eij} U_f \left(\frac{\partial K}{\partial F} \right) \left\{ \left(\frac{\partial F}{\partial I_{1e}} \right) - \frac{2}{3} \left(\frac{J_{2e}}{J_{3e}} \right)^2 \left(\frac{\partial F}{\partial J_{3e}} \right) \right\} \right] \delta_{kl} + 2G_0\rho_{eij} U_f \left(\frac{\partial K}{\partial F} \right) \left[\left(\frac{\partial F}{\partial J_{2e}} \right) \frac{\rho_{ekl}}{2J_{2e}} + \left(\frac{\partial F}{\partial J_{3e}} \right) \frac{\rho_{eklm}\rho_{elm}}{3J_{3e}^2} \right] \dots\dots\dots (5b)$$

$$U_f = 1, \text{ when } F = F_{\max} \text{ and } dF \geq 0$$

$$U_f = 0, \text{ otherwise}$$

Similarly, by combining Eq.(3) and Eq.(4), the authors derived the following plasticity equation³⁾ as,

$$d\varepsilon_{pji} = L_{ijkl} d\varepsilon_{ekl} \dots\dots\dots (6a)$$

$$L_{ijkl} = \left(\frac{\rho_{eij}}{J_{2e}} + D\delta_{ij} \right) \left(\frac{dH}{dJ_{2e}} \right) \frac{U_p \rho_{ekl}}{2J_{2e}} \dots\dots\dots (6b)$$

$$U_p = 1, \text{ when } J_{2e} = J_{2e\max} \text{ and } dJ_{2e} \geq 0$$

$$U_p = 0, \text{ otherwise}$$

The main objective of this paper is to combine the fracturing elasticity and the plasticity of the damaged concrete. In both cases, the control parameters are specified as the elastic strain to represent the internal stress intensity as shown in Fig.2. There exist other attempts to combine the plasticity and the continuum damage^{11),12)} where the

damage and plasticity were formulated with respect to the total stress and strain. Since the internal stress intensity as the driving action to the damage and plasticity is not explicitly adopted, the physical meaning for plastic and fracture surfaces (functions) used becomes vague. On the other hand, the elasticity regarded as the direct proportional value to internal stress intensity is the main feature of this modeling. For structural analyses, the total strain has to explicitly appear in the final constitutive equation. According to the deformational compatibility, we have,

$$d\varepsilon_{ij} = d\varepsilon_{eij} + d\varepsilon_{pji} \dots\dots\dots (7)$$

The combination of Eq.(5), Eq.(6) and Eq.(7) yields the full incremental constitutive equation. The matrix form of the combined elasto-plastic and fracture model is lastly brought to completion as,

$$d\{\sigma\} = [M]([I] + [L])^{-1} d\{\varepsilon\} \dots\dots\dots (8)$$

where $[M]$ and $[L]$ express the fracture and plasticity matrix to the fourth order tensors M_{ijkl} and L_{ijkl} . It may be hard to derive the full fourth order tensorial expression on the total stress-strain incremental relation in Eq.(8), because the non-symmetry of matrix L arises due to the presence of dilatancy.

3. MATERIAL CONSTANTS AND FUNCTIONS

(1) Concrete

From 2D and 3D cyclic loading data, the following four material functions on the continuum fracture and plasticity are proposed for concrete with normal aggregate and strength ranging from 15MPa to 50MPa^{2),3)} as,

$$K = K(F) = \exp \left[-\frac{F}{3.25} \left\{ 1 - \exp \left(-\frac{F}{0.8} \right) \right\} \right] \dots\dots\dots (9)$$

$$F = F(I_{1e}, J_{2e}, J_{3e}) = \frac{\sqrt{2}J_{2e}}{0.23\varepsilon_0 - \sqrt{3}I_{1e}} \cdot \frac{1}{5} \left\{ \frac{3\sqrt{3}}{2} \left(\frac{J_{3e}}{J_{2e}} \right)^3 + 6 \right\} \dots\dots\dots (10)$$

$$H = H(J_{2e}) = \frac{9}{10} \varepsilon_0 \left(\frac{J_{2e}}{\varepsilon_0} \right)^3 \dots\dots\dots (11)$$

$$D = D(I_{1e}, K) = \frac{(-1 + 2\nu_0)}{\sqrt{3}(1 + \nu_0)} 4K^2 + \frac{\sqrt{2}I_{1e} + 0.38\varepsilon_0}{0.28\varepsilon_0} (1 - 4K^2) \dots\dots\dots (12)$$

where,

$$\varepsilon_0 = 1.6(1 + \nu_0) \frac{f'_c}{E_0}$$

The above equations include the material constant ε_0 which was adopted so that those material

functions would be applicable to the normal aggregate and strength concrete.

The fracture function K represents the degradation of the shear elastic strain energy of concrete including defects. The parameter F is the indicator to express the macroscopic intensity of internal stress which advances the damage under arbitrary level of confinement. The function H indicates the plastic hardening of the internal plastic element in the damaged concrete (See Fig.2). The derivative D indicates the plastic dilatancy induced by the shear plastic dislocation along internal defects.

(2) Steel

The 3D constitutive law for steel is to be incorporated with the one for concrete when laterally confined concrete columns by steel are focused in analyses. This chapter will prove the general elasto-plastic and fracture model for concrete to cover the elasto-plastic behaviors for steel by the theory of plasticity incorporating Von-Mises yield function. Let the fracture parameter K remain constant ($= 1$). This means that the material concerned does not undergo any fracture (See Fig.2) with regard to the elastic strain energy. Further, the structural steel has no plastic dilatancy. The dilatancy derivative D has to be set null. By assuming unity and null for two functions, we have,

$$d\epsilon_{pij} = e_{eij} dg = \frac{S_{ij}}{2G_0} dg = s_{ij} dg' \dots\dots\dots (13)$$

$$dI_{1p} = 0 \dots\dots\dots (14)$$

where, dg and dg' are proportional coefficients. Since the fracture is ignored, the total stress itself indicates the intensity of the internal stresses directly. The incremental form of the plasticity is converted in terms of the stress tensors and Eq.(13) and Eq.(14) produce,

$$d\epsilon_{pij} = d\epsilon_{pij} + \delta_{ij} dI_{1p} = s_{ij} dg' \dots\dots\dots (15)$$

The differentiation of the second invariant of stress J_2 with respect to the total stress is proportional to the stress deviator. Then, we have another expression of Eq.(15) with the total stress tensors as,

$$d\epsilon_{pij} = \left(\frac{\partial J_2}{\partial \sigma_{ij}} \right) dg'' \dots\dots\dots (16)$$

The non-fracture and non-dilatancy assumptions are eventually equivalent to Eq.(16), which is the same with Prandtl-Reuss flow rule associated with exactly the Von-Mises plastic yield function applicable to the structural steel. It can be concluded that the flow rule for steel in the theory of plasticity is one of the particular cases of the proposed elasto-plastic and fracture model. The proportional coefficient dg'' specifies the magnitude of the plastic flow. In the plasticity, the rate of the plastic flow is determined by the plastic hardening rule⁸⁾. As for

the proposed model, the plastic hardening function H bears the role to actually specify the proportional coefficient in Eq.(16). The proposed plastic hardening model by Eq.(3) is converted to,

$$dJ_{2p} = \frac{dH}{dJ_{2e}} dJ_{2e} = \left\{ \frac{dH}{dJ_{2e}} \left(\frac{J_2}{2G_0} \right) \right\} d \left(\frac{J_2}{2G_0} \right) \dots (17)$$

According to the definition of the plastic second invariant by Eq.(3), we have the following another expression on the plastic rate provided the no dilatancy ($D = 0$) and no fracture ($K = 1$) in elasticity as,

$$\begin{aligned} dJ_{2p} &= \frac{e_{eij} d\epsilon_{pij}}{2J_{2e}} = \frac{S_{ij}}{2J_2} d\epsilon_{pij} \\ &= \frac{\sigma_{ij}}{2J_2} d\epsilon_{pij} - \frac{\sigma_{kk}}{2J_2} dI_{1p} \dots\dots\dots (18) \end{aligned}$$

Substituting Eq.(18) where dI_{1p} is equal to zero into Eq.(17), we have,

$$\begin{aligned} \sigma_{ij} d\epsilon_{pij} &= \frac{J_2}{G_0} \left\{ \frac{dH}{dJ_{2e}} \left(\frac{J_2}{2G_0} \right) \right\} dJ_2 \\ &= H' (J_2) dJ_2 \quad (= \text{plastic work}) \dots (19) \end{aligned}$$

The left side of Eq.(19) above indicates the total plastic work. The plastic work is equated with the increment of the plastic function represented by the second invariant of the stress as indicated by Eq.(19). This expression is exactly the same with the work hardening formulation of the plasticity⁸⁾. The function H is originally expressed by the elastic strain. But, provided no fracture, our function H is convertible to the hardening function H' which is controlled by the stress invariant used in the frame of plasticity as above. The proposed constitutive laws are proved to cover the conventional plasticity based on Von-Mises yield criterion.

4. EXPERIMENTAL VERIFICATION

It must be mentioned that the post failure behaviors (descending branch of the stress strain curve) are not covered by the model. Because, the continuum fracture model used is applicable only when the defects are spatially distributed with fewer localization. When we intend to expand the applicability, the fracture indicator should be size dependent, but at present, the formulation is not size dependent. Then, in the following computation, the authors stopped computation when the value of K reaches 0.35, which is supposed to be the tentative limit of the continuum fracture.

(1) Confined cylinder

Axial stress-strain relation of concrete cylinder encased by steel is shown in Fig.3. The constitutive equation is solved with the following condition of confinement by steel as,

$$\sigma'_{xx} = \sigma'_{yy} = \frac{1}{2} \rho \sigma_s (\epsilon_{xx}) \dots\dots\dots (20)$$

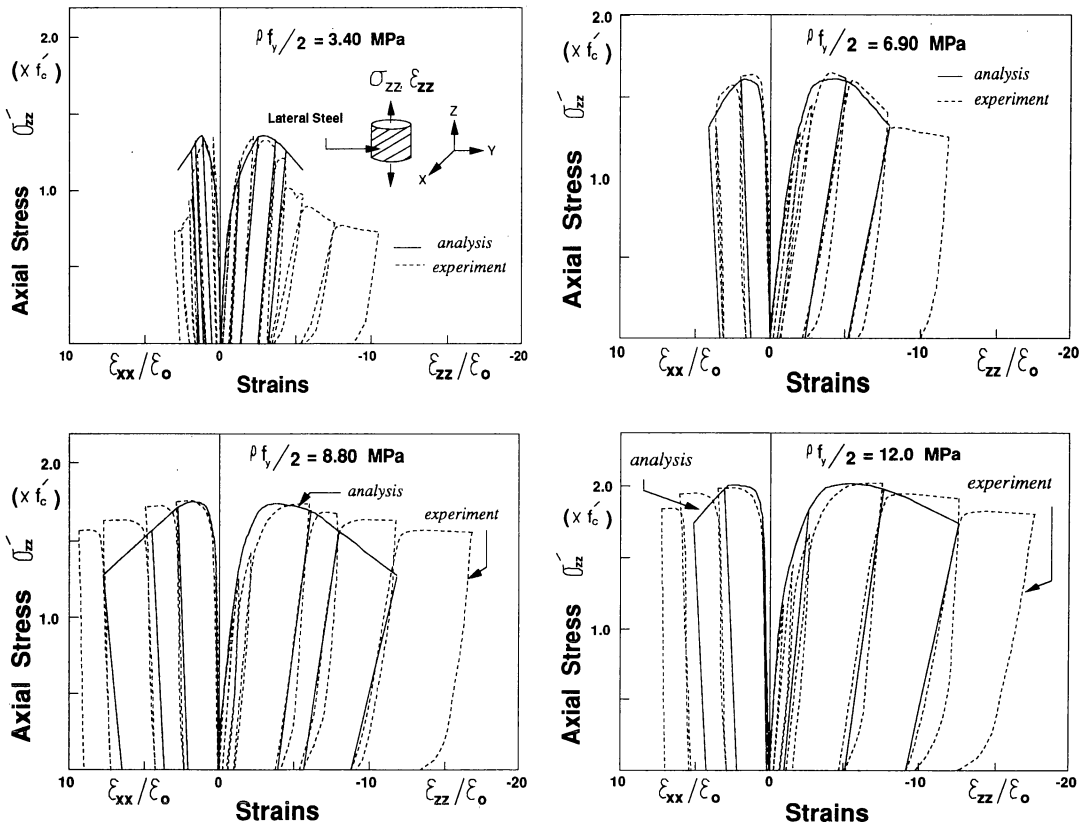


Fig.3 Stress-strain Relation of Steel Encased Cylinder : $f'_c = 29\text{MPa}$, $\epsilon_o = 0.0025$

where ρ is the volume ratio of steel encasing and σ_s is the hoop stress of steel associated with the lateral strain. According to the rule of notation which states that suffix ['] (prime) reverses sign of original stress and strain based variables, concrete stress σ' is positive when compression is designated.

The dilatancy modeling serves the lateral inelastic deformation which induces the lateral stress in turn as well as the fracture model. Not only the loading but the plastic residual strain fairly coincide with the experimental data. The monotonic loading curve of axial stress under constant lateral pressure ($\sigma_{xx} = \sigma_{yy}$) is shown in Fig.4. The prediction is performed by step-by-step integration. The analytical results are close to the experimental data performed by Richart⁵⁾ and Kotsovos⁶⁾. The precision of the strength of hydro-pressured concrete relies primarily on the fracture function. The above stress condition will be concern of structural analysts on confined RC columns. The core concrete of circular and/or rectangular sectional columns is thought to undergo the triaxial stress state similar to the loading in Fig.4.

(2) Failure envelope

The failure envelope on the stress space has been a principal target of triaxial loading tests undertaken in the past. This is because the obtained envelope were expected to be the plastic function within the frame of the plasticity.

However, it is comprehended that the failure envelope which exhibits the set of stress at failure will be the material behavior to be computed as a product of both the elasto-plasticity and the fracture. Fig.5 shows the computed failure curve located at different points on the equivolumetric stress plane named π plane^{2),8)}. The hydrostatic versus deviatoric failure curve is found to be affected by the effect of the third invariant on the continuum fracture. The plot of the failure was the peak stress which presents the zero tangential stiffness. This means that the failure surface is characterized by the singular state where the fracturing softening upsets the hardening owing to the plasticity. The computed result is near the experimental observation on both total stress planes. Both the plastic hardening and the fracture parameter are crucial for determination of the failure conditions.

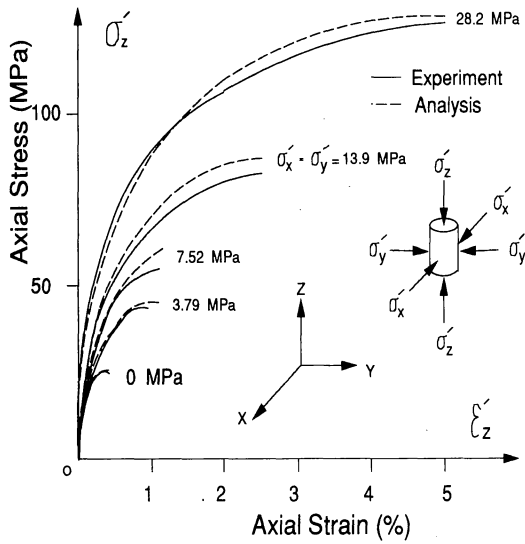


Fig.4a Stress-Strain Relation of Hydraulically Confined Cylinder⁵⁾.

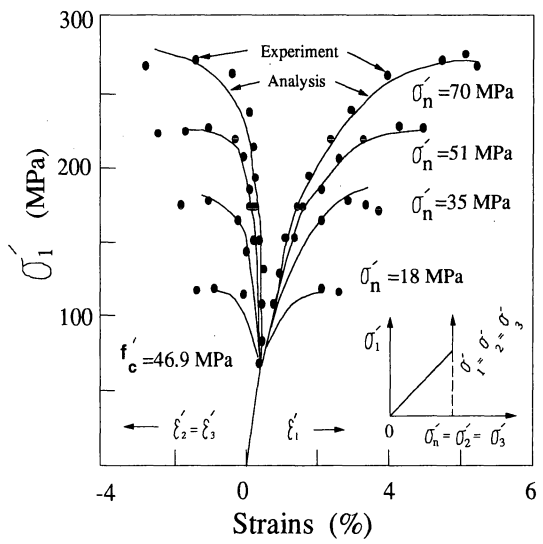


Fig.4b Stress-strain Relation of Hydraulically Confined Cylinder⁶⁾.

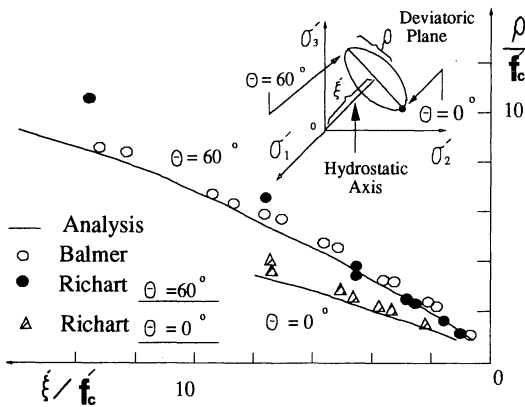


Fig.5 Failure Envelope on the Stress Space^{5),7),8)}

(3) Biaxial compression

The biaxial behavior is regarded as the general triaxial aspect viewed from the different angle. The access to the failure envelope was made mainly on the proportional loading paths in tests. The experiment by Kupfer et al.⁹⁾ and the prediction are shown in Fig.6, respectively. The biaxial failure surface is also a slice of the triaxial envelope. There observed are lesser discrepancy between the analysis and the experimental data.

The strain paths on the biaxial plane under the cyclic uniaxial stress are shown in Fig.7⁷⁾. When the stress exceeds approximately 90% of the strength, the strain path on loading gets oriented to the direction equivalent to greater Poisson's ratio in appearance. The larger Poisson's ratio in unloading, which cannot be idealized if within the frame of plasticity, is also found under uniaxial compress-

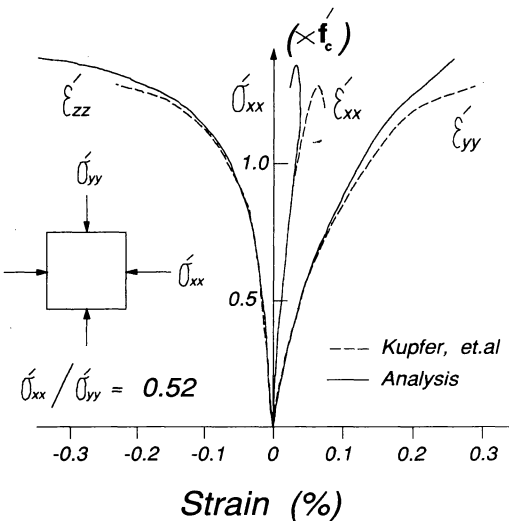
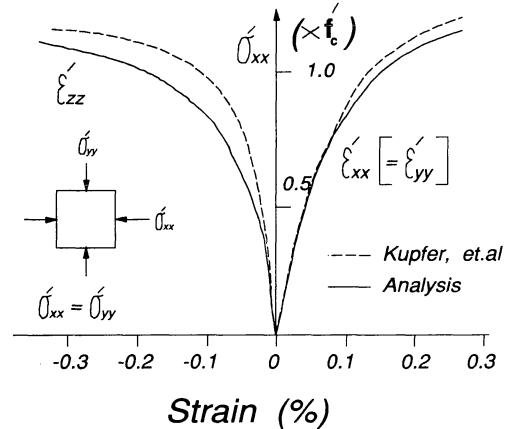


Fig.6a Isotropic and Anisotropic Biaxial Compression⁹⁾.

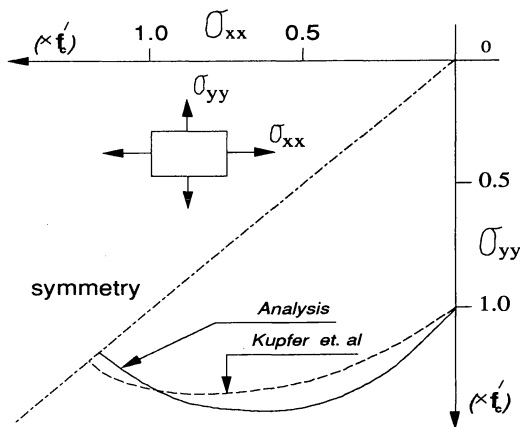


Fig.6b Biaxial Failure Envelope on the Stress Space⁹⁾.

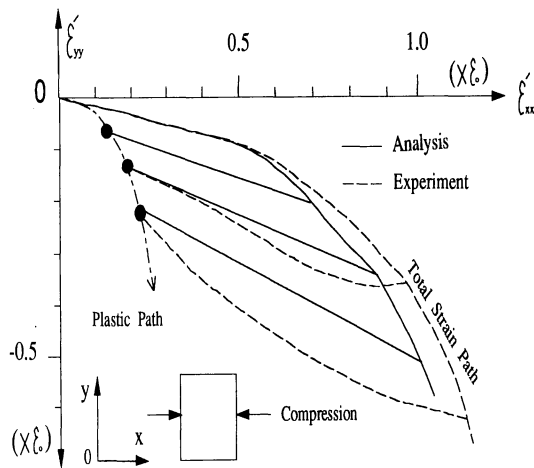


Fig.7 Biaxial Strain Path under Uniaxial Stress⁴⁾

ion. These behaviors are associated with the model of combined dilatancy and the fracture. The uniaxial and biaxial stress states are also our concern on the structural analysis of laterally confined concrete columns with rectangular sections. The concrete located near lateral ties is subjected to the stresses close to biaxial one.

(4) Loading path

The unloading path from the hydraulic compression was verified as shown in Fig.8¹⁰⁾. On this path, the progress of inelasticity (fracture and plasticity) and the elastic recovery take place simultaneously. As for this stress path, the models of elasticity, plasticity and fracture are mutually correlated. The analytical result appears to match the reality. In analysis, the initial elastic stiffness and Poisson's ratio were decided so that the initial computed stiffness coincides with the experimental data.

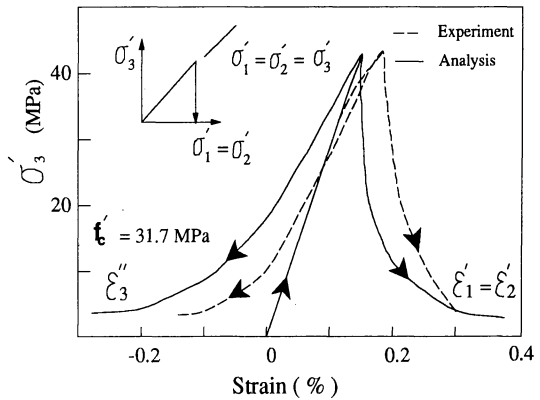


Fig.8 Unloading Path from the Hydraulic Compression¹⁰⁾

5. CONCLUSIONS

The constitutive laws of the continuum fracture and the plasticity on the damaged continuum were combined under the triaxial stress state, and the material functions and coefficients were proposed for normal aggregate concrete having 15-50 MPa of the uniaxial compressive strength. The full constitutive equation in terms of the stiffness matrix was accomplished in the incremental form of the total stress and strain tensors. In this process, the elastic strain which was utilized as the main parameter to decide the plasticity and fracture was treated as the intermediate parameter.

The experimental verification was carried out concerning the stress-strain of steel encased cylinders, failure envelopes computed and loading paths and strain responses. The strength specified by the loading path was not incorporated in formulation but computed as the combination of plastic hardening and the fracturing softening of elasticity. Then, the comparison of computed triaxial strength with the real strength became the check of plasticity as well as fracturing models used. The versatility of the model proposed was examined. The formulated elasto-plastic and fracture model proved to cover the classical theory of plasticity linked to the Von-Mises yield function and the well known associated flow rule by Prandtl-Reuss.

The development of the triaxial model here was motivated by the needs of confined RC column analysis. The model finalized hereby will be utilized as a micro model in FEM for analyzing the confinement effect by the lateral steel. The spacing of lateral hoops, way of arranging intermediate ties and the shape of cross section, which are supposed to be influencing factors on the strength and ductility of RC columns, will be taken into account in the structural analysis. The verification will be

performed again in the structural members level.
ACKNOWLEDGMENT : The authors express their gratitude to Prof. H. Okamura, The University of Tokyo for valuable discussion and guidance. The first author is grateful to Japan International Cooperation Agency for their financial support granted when the author served as a Faculty in Asian Institute of Technology.

REFERENCES

- 1) Sugano, T., Inoue, N., Koshika, N., Hironaka, Y. and Hayami, K. : 3-Dimensional Nonlinear Analysis of Reinforced Concrete Columns under Repeated Bending and Shearing Forces, Proceedings of JCI 2nd Colloquium on Shear Analysis of RC Structures, Japan Concrete Institute, Vol.JCI-C5, pp.87~96, October 1983.
- 2) Maekawa, K., Takemura, J., Irawan, P. and Irie, M. : Continuum Fracture in Concrete Nonlinearity under Triaxial Confinement, Proc. of JSCE, No.460/V-18, 1993.
- 3) Maekawa, K., Takemura, J., Irawan, P. and Irie, M. : Plasticity in Concrete Nonlinearity under Triaxial Confinement, Proc. of JSCE, No.460/V-18, 1993.
- 4) Maekawa, K. and Okamura, H. : The Deformational Behavior and Constitutive Equations for Concrete Using Elasto-Plastic and Fracture Model, Journal of the Faculty of Engineering, The University of Tokyo (B), Vol.XXX-VII, No.2, 1983.
- 5) Richart, F.E., Brandizaeg, A. and Brown, R.L. : A Study of the Failure of Concrete under Combined Compressive Stresses, University of Illinois, Engineering Experimental Station, Bulletin No.185, p.104, 1928.
- 6) Kotsovos, M.D. and Newman, J.B. : Mathematical Description of Deformational Behavior of Concrete under Generalized Stress Beyond Ultimate Strength, Journal of ACI, Vol.77, No.5, pp.340~346, October, 1980.
- 7) Balmer, G.G. : Shearing Strength of Concrete under High Triaxial Stress-Computation of Mohr's Envelope as a Curve, Structural Research Laboratory Report No.SP-23, Bureau of Reclamation, United States Department of the Interior, 1949.
- 8) Chen, W.F. and Saleeb, A.F. : Constitutive Equations for Engineering Materials, Vol.1, John Wiley & Sons, Inc., 1982.
- 9) Kupfer, H., Hilsdorf, H.K. and Rusch, H. : Behavior of Concrete under Biaxial Stress, Journal of ACI, Vol.66, No.8, pp.656~666, August 1969.
- 10) Kotsovos, M.D. and Newman, J.B. : Mathematical Description of Deformational Behavior of Concrete under Complex Loading, Magazine of Concrete Research, Vol.31, No.107, pp.77~90, June, 1979.
- 11) Ju, J.W. : On Energy Based Coupled Elasto-Plastic Damage Theories-Constitutive Modeling and Computational Aspects-, Int. Journal of Solids and Structures, Vol.25, pp.803~833, 1989.
- 12) Bazant, Z.P. and Kim, S. : Plastic Fracturing Theory for Concrete, Journal of Engineering Mechanics, ASCE, Vol.105, No.EM3, June, 1979.
- 13) Research and Surveying Report on the Mechanical Properties of Concrete. Chapter 2, Constitutive Laws of Concrete, Concrete Library, No.69, JSCE, August, 1991.
- 14) Committee Report on Ductility of Concrete Structures and Its Evaluation, Japan Concrete Institute, Vol.JCI-C12, March, 1988.

(Received October 16, 1991)

三軸応力下におけるコンクリートの弾塑性破壊モデル

前川宏一・竹村淳一・Paulus IRAWAN・入江正明

空間的に分散した損傷を内在するコンクリート連続体に対して、弾性ひずみを主パラメータとする塑性モデルと損傷弾性モデルを結合し、完備した構成式を導出した。さらに、三軸載荷実験結果を用いて多角的視点からモデルの検証を行った。また、本モデルが塑性関数を基準とする弾塑性理論をも包含した、より一般化された構成式であることを示すとともに、横拘束鉄筋を有するRC柱の応力解析に必要な予測精度を有していることを実証した。